

# Role of PKA Spectrum and PKA Density in Defect Production and Implications for H-isotope Trapping in Tungsten

Friday 14 May 2021 18:25 (20 minutes)

Tungsten is an attractive choice for armour material for divertors in fusion reactors, but a globally recognized concern is that the accumulated radiation damage by 14.1 MeV neutrons can significantly enhance its otherwise low H-isotope affinity [ 1]. Lack of a high flux 14.1 MeV neutron source, inaccessibility of the reactor-like conditions and the inherently complex material response to neutrons have kept this area active for a long time. This has triggered rigorous modelling efforts which will require extensive experimental benchmark with ion as well as low energy neutron irradiation experiments for credible projections [ 2, 3, 4,5,6,7,8]. It is widely accepted that the total dpa cannot be the only parameter for comparison [9,10,11,12,13,14]. The recoil energy spectrum (PKA spectrum) and recoil density can play a significant role in the defect-structure formation, but there exists no systematic study of their correlation. This is of utmost importance in the case of fuel retention since the H-trapping is intimately correlated with the type and the quantity of the defects [15,16]. This paper addresses two questions in the context of trapping: (1) what is the effect of PKA spectrum on the defect structure formation? and (2) what is the influence of PKA density in the final defect structure? The first point is addressed by experiments with similar PKA spectrum for the same dpa by using 10 MeV boron ions and 3.5 MeV helium ions and is compared with previously reported heavy-ion irradiation experiments [17]. The PKA spectrum produced by different ions used in experiments is shown in Fig.1. It can be seen that it is broadly similar to that created by fusion neutrons. For comparison, the PKA spectrum of 250 keV helium is also shown which has a much lower PKA energy.

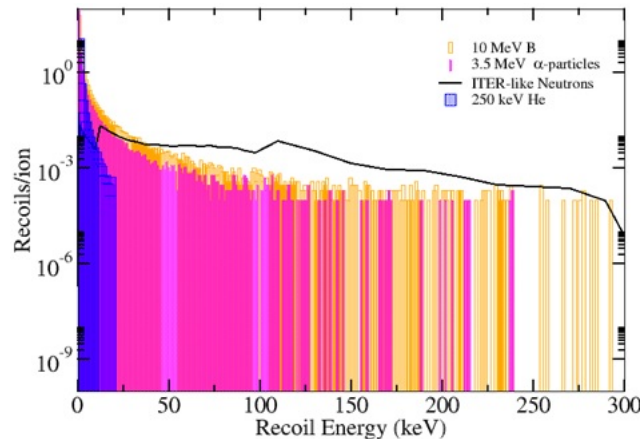


Fig. 1: PKA spectrum of various ions and neutrons

Figure 1:

The second point is addressed by using a combination of modelling and experiments where, similar PKA spectrum with different recoil densities are used. The recoil density (or 'in-cascade density' of recoils) is defined for a typical cascade volume as  $\rho_{pka} = Npka/V$  ( $V = \pi r^2 h$ ,  $h$  = range,  $r$  =lateral width). The results indicate that  $\rho_{pka}$  is a key factor in deciding the damage structure and their size distribution. The recoil density for 10 MeV B  $\sim 10^{19} \text{ m}^{-3}$ , 3.5 MeV He  $\sim 10^{18} \text{ m}^{-3}$  and for heavy ions (1-80 MeV W) varies between  $10^{23}$  and  $10^{20} \text{ m}^{-3}$  respectively. For 250 keV He irradiation it is  $\sim 10^{20} \text{ m}^{-3}$  which is similar to heavy ion irradiation. The experimental observations motivate a model for a collective defect interaction to understand the final defect structure. For a given projectile each PKA produces individual cascades that leaves behind immobile and mobile defects and it is hypothesized that the immobile defects compete to capture the mobile defects. This Competitive-Capture Model (CCM) includes various interactions among defects implemented in a 2D-Monte Carlo scheme. The defect population corresponding to each PKA energy is taken from MD simulations at the end of the cascade. The defects are distributed corresponding to the inter-PKA distance mapped on to the 2D surface and their evolution is studied as a function of time. The model not only explains the fluence

dependence of defect structures in a semi-quantitative way but also allows projections for neutron irradiation where the  $\rho_{pka}$  is comparatively much smaller.

The irradiation experiments were done on recrystallized tungsten foils of  $8 \times 8 \times 0.1 \text{ mm}^3$  size as shown in Table.1. Post and pre-irradiation characterization was done by TEM, PAS and SEM for defects and surface morphology.

Ion (mass)	E (MeV)	Mean Range (mm)	Fluence (ions/m <sup>2</sup> )	Dpa (Ed = 90 eV)
He <sup>2+</sup> (4)	3.5	5.1	$8.7 \times 10^{18}$	0.001
He <sup>2+</sup> (4)	3.5	5.1	$9.1 \times 10^{19}$	0.01
He <sup>2+</sup> (4)	3.5	5.1	$1.8 \times 10^{20}$	0.02
B <sup>3+</sup> (11)	10	4.1	$1.3 \times 10^{18}$	0.001
B <sup>3+</sup> (11)	10	4.1	$1 \times 10^{19}$	0.01
He <sup>+</sup> (4)	0.25	0.6	$5 \times 10^{19}$	0.022

**Table.1. Irradiation Parameters**

Figure 2:

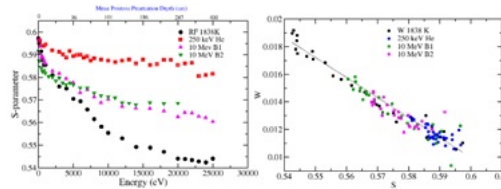


**Fig.2: S-E and S-W curves of various samples**

Figure 3:

The positron lifetime data showed that boron irradiation forms predominantly single vacancies (~200 ps) at room temperature. Neutron irradiation for similar dpa also reported single vacancy formation [8] confirming that the similarity of PKA spectrum is playing a role. In line with previously reported experiments [18], it is seen that the 250 keV He-ions also produce single vacancies as inferred from the S-W curve in Fig.2. However, the depth profile of the defects, characterized using S-parameter shows a saturation in the case of helium in contrast to boron. This conclusively show that almost all low mass ions predominantly form single vacancies which is a direct consequence of the PKA spectrum. A semi-quantitative analysis of the defect density formed in various irradiated samples will be presented.

The TEM analysis of the boron and helium irradiated samples (Fig.3) shows the significance of PKA density in the meso-scale defect formation. While boron forms larger defects up to 35 nm, helium shows smaller defects (<12 nm). Surprisingly, this is also close to the previously reported heavy ion irradiation experiments [17,19] despite the difference in PKA spectra. These results can be understood from the difference in PKA density using the CCM. Interestingly, for 80 keV He-irradiation, Zhao et al., had reported the formation of defect clusters of similar size at room temperature [20] which can also be explained by the same model. Detailed analysis of 3.5 MeV helium, which has a much lower PKA density will be presented in the paper.

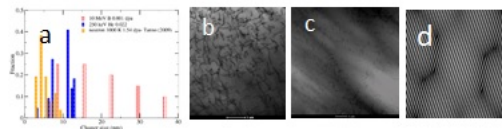


**Fig.3: (a) defect size distribution, (b) B-irradiated, (c) He-irradiated (d) HRTEM of He-irradiated (250 keV)**

Figure 4:

These results conclusively indicate the role of PKA spectrum and PKA density in the defect structure formation. While vacancy defects depend only on the PKA spectrum at moderate fluences, the meso-scale defects observed in TEM depend on their density. A detailed analysis of the vacancy population and corresponding defect densities will be presented for different irradiation scenarios discussed here. Deuterium diffusion and trapping for different defect population will be discussed.

The present work suggests low-mass, high fluence experiments are more suitable for simulating neutron induced defect structures in the context of fuel trapping. It has to be noted that the present experiments are at room temperature. In a reactor the first-wall and the divertor will be at higher temperature. Ideas for extrapolating results to reactor relevant conditions and the possible experiments will be presented.

Part of this work was completed under IAEA-CRP agreement number 18183/R0.

#### References:

- [ 1] <https://www-amdis.iaea.org/CRP/IrradiatedTungsten/>
- [ 2] Nordlund et al., Nature Commun. 2019, 9:1084 and references therein
- [ 3] S.L. Dudarev et al., Nucl. Fusion. 2018, 58 126002
- [ 4] Wirth et al., J. Mater. Res., 2015, 30(09), 1440
- [5] A.E. Sand et al., Mater. Res. Lett., 2017 5, 357-363
- [6] Golubov et al., Comprehensive Nuclear Materials, Elsevier 2012 ISBN: 978-0-08-056027-4
- [7] O. El-Atwani et al., Acta Materialia, 2018, 149, 206
- [8] Shimada et al., 2015 Nucl. Fusion 55 013008
- [9] Li et al., Phil. Magazine 2012, 92(16), 2048
- [10] G. Was, Fundamentals of radiation material science, Springer Berlin, 2007
- [11] S. Zinkle, Comprehensive Nuclear Materials, Elsevier 2012 ISBN: 978-0-08-056027-4
- [12] Abernethy R.G. 2017 Mater. Sci. Technol. 33 388 and references therein
- [13] S. Ishino. J. Nucl. Sci. and Technol. 1989, 26:1, 137
- [14] Gilbert et al., J. Nucl. Mater., 2015, 467, 121-134
- [15] Watanabe et al., J. Nucl. Mater., 2014, 455, 51-55
- [16] Samolyuk et al., Fusion Tech. 2017, 71:1, 52
- [17] P.N. Maya et al 2019 Nucl. Fusion 59 076034
- [18] A. Dabelle et al., J. Nucl. Mater., 2007, 362, 181
- [19] P. Sharma et al., 2019 Microscopy and Microanalysis, 25(6), 1442-1448.
- [20] Zhao et al., Nucl. Inst. Methods. B, 2018, B414, 121

## Country or International Organization

India

## Affiliation

Institute for Plasma Research, Bhat, Gandhinagar 382428, Gujarat, India

**Author:** MAYA, P.N (Institute for Plasma Research, Bhat, Gandhinagar, India)

**Co-authors:** SHARMA, Prashant (ITER-India, IPR Gandhinagar); Dr MUKHERJEE, Saurabh (Bhabha Atomic Research Center, Trombay, Mumbai, 400085, India); AKKIREDDY, Satyaprasad (Institute for Plasma Research); Dr BALAJI, S (Indira Gandhi Center for Atomic Research, Kalpakkam, India); Dr DAVID, C (Indira Gandhi Center for Atomic Research, Kalpakkam, India); Dr GAUTAM, Abhay Raj (Indian Institute of Technology, Gandhinagar, Gujarat, India); Ms KIKANI, Purvi (Institute for Plasma Research, Bhat, Gandhinagar, 382428, Gujarat, India); Dr PUJARI, P K (Bhabha Atomic Research Center, Trombay, Mumbai, India); DESHPANDE, Shishir (Institute for Plasma research)

**Presenter:** MAYA, P.N (Institute for Plasma Research, Bhat, Gandhinagar, India)

**Session Classification:** P8 Posters 8

**Track Classification:** Fusion Energy Technology